Eur. Phys. J. B (2019) 92: 183
https://doi.org/10.1140/epjb/e2019-100137-7

THE EUROPEAN PHYSICAL JOURNAL B

Regular Article

The structural transition under densification and the relationship between structure and density of silica glass

N.V. Hong[1], L.T. Vinh[2,3,a], P.K. Hung[1], M.V. Dung[4,5], and N.V. Yen[6]

[1] Department of Computational Physics, Hanoi University of Science and Technology, Hanoi, Viet Nam
[2] Simulation in Materials Science Research Group, Advanced Institute of Materials Science, Ton Duc Thang University, Ho Chi Minh City, Viet Nam
[3] Faculty of Electrical and Electronics Engineering, Ton Duc Thang University, Ho Chi Minh City, Viet Nam
[4] Institute of Applied Materials Science, Vietnam Academy of Science and Technology, No. 1A TL29 Str., Thanh Loc Ward, District 12, Ho Chi Minh City, Viet Nam
[5] Thu Dau Mot University, Binh Duong Province, Viet Nam
[6] Institute of Research and Development, Duy Tan University, Da Nang 550000, Viet Nam

Received 8 March 2019 / Received in final form 2 June 2019
Published online 26 August 2019

Abstract. The structure of silica glass (SiO_2) at different densities and at temperatures of 500 K is investigated by molecular dynamics simulation. Results reveal that at density of 3.317 g/cm^3, the structure of silica glass mainly comprises two phases: SiO_4- and SiO_5-phases. With the increase of density, the structure tends to transform from SiO_4-phase into SiO_6-phase. At density of 3.582 g/cm^3, the structure comprises three phases: SiO_4- , SiO_5-, and SiO_6-phases, however, the SiO_5- phase is dominant. At higher density (3.994 g/cm^3), the structure mainly consists of two main phases: SiO_5- and SiO_6-phases. In the SiO_4-phase, the SiO_4 units mainly link to each other via corner-sharing bonds. In the SiO_5-phase, the SiO_5 units link to each other via both corner- and edge-sharing bonds. For SiO_6-phase, the SiO_6 units can link to each other via corner-, edge-, and face-sharing bonds. The SiO_4-, SiO_5-, and SiO_6-phases form SiO_4- SiO_5- and SiO_6-grains respectively and they are not distributed uniformly in model. This results in the polymorphism in the silica glass at high density.

1 Introduction

Information about the structure and properties of silica glass (SiO_2) is very important in the geophysics and materials science fields. So, silica as well as silicate glasses are interesting to scientists in the areas of physics and materials science. Investigating the structure of silica glass is expected to clarify the physical properties and behavior of Si–O network structure [1–7] under the changes of pressure and temperature. At low pressure, the relatively-rigid SiO_4 tetrahedron is the basic structural unit in silica/silicate glasses and melts: each Si connects to four nearest neighbor O atoms, with Si–O bond length of approximately 1.62 Å, and each O links to two nearest neighbor Si atoms [8–11]. The Si–O–Si bond angle is very flexible and distributes in a 120–180° wide-range with the peak at around 144° which shows the structural differences of silica/silicate glasses in comparison to crystalline forms. Besides, the O–Si–O angles distribution in relatively-rigid SiO_4 tetrahedra has the peak at around 105–109° and these SiO_4 tetrahedra link to each other forming a continuous random network in 3D space [12–16]. MD simulation using the semi-empirical interatomic potentials [9–11,17–20] reproduces well the samples of silica and silicate glasses/melts with the characteristics in good agreement with experimental data. Simulations in works [5,21,22] reveals that the silica/silicates show several anomalies including: density anomaly, diffusion anomaly, spinodal instability and structural phase transition. As the silica/silicates are densified, the system gradually transforms from tetrahedral- to octahedral-network structure. As having revealed in works [9,11,23,24], the topology of SiO_x tetrahedra is identical and not dependent on pressure. By *ab* initio simulation [25,26], structural characteristics show the good agreement with data of diffraction experiments and reveal the presence of strong directional bonds. Meanwhile, the study [25] shows no evidence of the density-anomaly for a wide temperature range. Short-range and intermediate-range order are characterized by Si–O bond length, O–Si–O and Si–O–Si bond-angle distributions, and statistics of the nearest neighbors as well as voronoi polygon and simplex statistics [27–29]. The advantage of the voronoi polygon and simplex methods is not dependent on cut off distance.

[a] e-mail: lethevinh@tdtu.edu.vn

However, it is difficult to show the relationship between structural characteristics and density of the model. The flexibility of the network structure is an important condition of existence of many different glass states. This explains for the specific glass-forming properties of SiO_2 and for the very low ability of transition from amorphous states to crystalline. It has been shown that, Silica has four major polymorphs: Cristobalite, Tridymite, Quartz and glass. A lot of theoretical calculations, computer simulation and experimental measures concerning with the behavior of various high-pressure silica phases (keatite, coesite, stishovite, $CaCl_2$-, a-PbO_2-, I2/a, baddeleyite, fluorite, and pyrite(Pa-3)-types) [4–6] have been carried out for many decades. Total energy calculations using ab initio method for specific structures have provided an explanation for structural transformation from amorphous to crystalline silica [30]. However, the experimental evidence of phase boundaries is still in debate and many results were contradictory among different publications on structural phase transition at high pressures [31–33]. Liquid–liquid phase transition, which results in the regions with different densities in liquid system as temperature or pressure are varied. Namely, the phase transition from low density (LD) to high-density (HD) form has also been shown by experiments and molecular dynamics simulation [5,34–50] for H_2O, Si, SiO_2, Al_2O_3-Y_2O_3, ... The polyamorphism was first recognized in the H_2O system. Under compression at temperature of 77 K, amorphous ice transforms from LD to HD state at 0.60 Å ± 0.05 GPa [36]. Some strong experimental evidences suggesting a liquid-liquid transition in water are obtained from glassy water. Especially, many experiments show the presence of two distinct glassy states (LD and HD states) which can be reversibly interconverted by the application (or removal) of pressure [36–41].

For amorphous silica, the polyamorphism also was shown by both experiments [42,43] and by computer simulations [44,50]. The polyamorphism as well as LD-HD transition has been study for a long time, however the relation between structural characteristics and densities of LD/HD phases are still an open question.

In this work, the structure and structural transformation of silica glass under densification will be investigated via analyzing SiO_x-network structure. The connection between SiO_x in silica network as well as the clustering of SiO_4, SiO_5 and SiO_6 units forming SiO_x-grains will be reported. Specially, the relationship between structure and density that is shown via characteristics of pair radial distribution function (PRDF) will be clarified and explained in detail. The correlation between density and structural characteristics that can be observed from RPDF will support the technique to determine the density from structure and vice versa.

2 Calculation method

Silica model consisting of 1666 Si and 3332 O atoms at temperature of 500 K and at different densities is constructed by means of MD simulation using BKS potentials and periodic boundary condition. Despite of being simple pairwise potentials, BKS potentials can produce silica models with structural characteristics in good agreement with experiments and ab-initio calculation. The BKS models have played a significant role in study the structure of silica and been applied in numerous works for a long time. Namely, the BKS models have been applied in studies of structural phase transition under compression, the structural phase transformation of quartz [33–35], the polymorphism, the LD–HD phase transition, phase separation in amorphous/melts silica [36–40]. Because of their simple, the BKS potentials are appropriate for studying the structure of silica models with the rather large size.

In this simulation, to integrate the equation of motion, the Verlet algorithm is applied with MD step of 1.0 fs. The initial configuration of silica model with density 2.20 g/cm^3 (corresponding to real density of amorphous silica at ambient pressure and temperature) is generated by placing all atoms randomly in a simulation box. After that, the initial model is heated up to 6000 K to remove initial configuration. Next the model is cooled down to 5000, 4000, 3000, 2000, 1000 and finally 500 K with the cooling rate of 2.5 K/ps. At each temperature, the model is relaxed for 10^5 MD steps. Next, a long relaxation (10^7 MD steps) has been done to get equilibrium state using isothermal-isobaric (NPT) ensemble (in the isothermal-isobaric ensemble, the number of atoms (N), pressure (P) and temperature (T) are constant). Next, the model is compressed to different pressures (5, 8 and 19 GPa) to get models M1, M2 and M3 with densities of 3.317, 3.584 and 3.993 g/cm^3 respectively. Finally, the models M1, M2, and M3 are relaxed in 10^7 MD steps to get equilibrium state using NPT ensemble.

Table 1. The model of amorphous SiO_2 at different density at 500 K.

Model	M1	M2	M3
Density	3.317	3.582	3.994

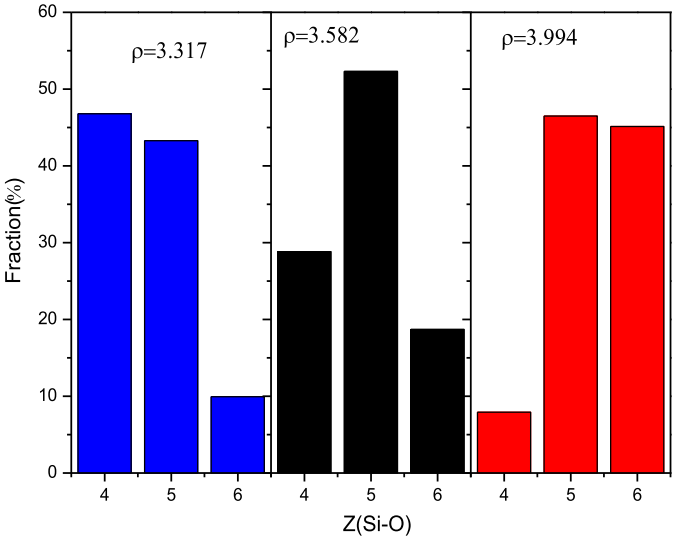

Fig. 1. Distribution of SiO_x coordination units at three different densities.

Table 2. Size-distribution of the SiO_x-cluster: Ncl is the number of clusters; Na is the number of atoms in the cluster.

ρ	3.317		3.582		3.994	
	Ncl	Na	Ncl	Na	Ncl	Na
	45	5	117	5	96	5
	17	9	30	9	18	9
	9	13	19	13	3	13
SiO_4	1	17	1	16	1	21
	3	21	9	17		
	2	45	4	21		
	1	77	1	24	8	6
	1	2549	2	25	1	10
			3	29	1	3413
	1	20	2	33		
SiO_5	1	22	1	36		
	1	2782	1	41	3	7
			1	45	2	13
			1	76	1	3287
	50	7	1	88		
	2	11	1	124		
	3	12	1	141		
	4	13				
	4	16	2	6		
SiO_6	2	17	1	11		
	2	18	1	21		
	1	21	1	3549		
	1	22				
	1	23	45	7		
	1	25	3	11		
	2	27	8	12		
	1	30	5	13		
	1	42	1	15		
	1	72	2	16		
			1	19		
			1	20		
			2	22		
			2	23		
			1	24		
			1	26		
			1	27		
			1	28		
			1	36		
			1	39		
			1	41		
			1	43		
			1	44		
			1	53		
			1	63		
			1	98		
			1	117		
			1	160		
			1	252		

The structural data of considered models is determined by averaging over 1000 configurations during the last 10^4 MD steps. To identify SiO_x coordination units, the Si–O cutoff radius chosen is the first minimum position of the Si–O pair radial distribution function with value of 2.30 Å. Size distribution of SiO_4-, SiO_5- and SiO_6-clusters is calculated by following algorithm: (1) the SiO_x units is calculate and decomposed into three sets: SiO_4-, SiO_5- and SiO_6-ones; (2) in the set of SiO_4 units, all units are labeled from 1 to n (n is the number of SiO_4 units, the Si and O atoms in one SiO_x have the same label). After that, if two SiO_4 units have at least one common O atom then they will belong to the same cluster and have the same label (value of this common label is the label of the unit with smaller value). Finally, the units with the same label will belong to one cluster. For the set of SiO_5 and SiO_6 units, the calculation of size-distribution is conducted similarly to that for SiO_4-set. The calculation of SiO_x clusters also uses the boundary condition the same as the calculation of coordination units.

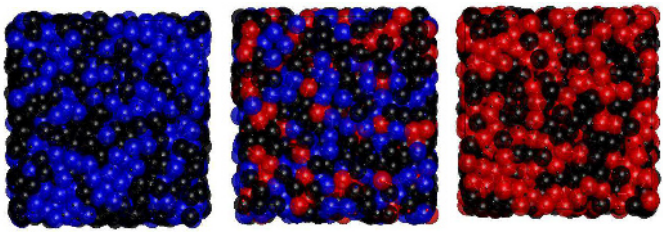

Fig. 2. Distribution of SiO_4-, SiO_5- and SiO_6-domains in silica glass at density of 3.317, 3.582, 3.994 g/cm^3 corresponding from left to right. The SiO_4 in blue, SiO_5 in black, SiO_6 in red.

3 Results and discussion

Table 1 shows the density of SiO_2 models at temperature of 500 K. The models M1, M2 and M3 have density of 3.317, 3.582 and 3.994 g/cm^3 respectively. The densities are chosen to assure that: in model M1, most of SiO_x coordination units are SiO_4 and SiO_5; in model M2, most of SiO_x are SiO_5 but it also exists a significant fraction of SiO_4 and SiO_6; in model M3, most of SiO_x are SiO_5 and SiO_6.

Figure 1 shows the distribution of SiO_x coordination units as a function of density. At density of 3.317 g/cm^3, the fraction of SiO_4, SiO_5, and SiO_6 is 47, 43 and 10% respectively. At density of 3.582 g/cm^3, the fraction of SiO_4, SiO_5, and SiO_6 is 29, 52 and 19% respectively. It reveals that as the density increases from 3.317 to 3.582 g/cm^3, the SiO_4 coordination units tend to transform to SiO_5; SiO_5 coordination tends to transform to SiO_6. At density of 3.994 g/cm^3, fraction of SiO_4, SiO_5, and SiO_6 is 8, 47 and 45% respectively. At high pressure, most of SiO_x coordination units are SiO_5 and SiO_6. It means that, the SiO_4 units are stable at low density/pressure. In contrast, the SO_5 and SiO_6 units are stable at high density/pressure. As density/pressure increases, the SiO_4 units tend to transform into SiO_5 and SiO_6. To clarify the spatial distribution (arrangement) of SiO_x in model as well as the link amongst SiO_x, we have investigated the size distribution of SiO_x clusters/subnets.

Table 2 shows the size-distribution of the SiO_x-clusters. It can be seen that at density of 3.317 g/cm^3. The SiO_5 coordination units form three cluster with size of 20, 22 and 2782 atoms. The SiO_4 coordination units form a large cluster of 2549 atoms and many small clusters with size from 5 to 77 atoms. The clusters with size of 5 atoms are

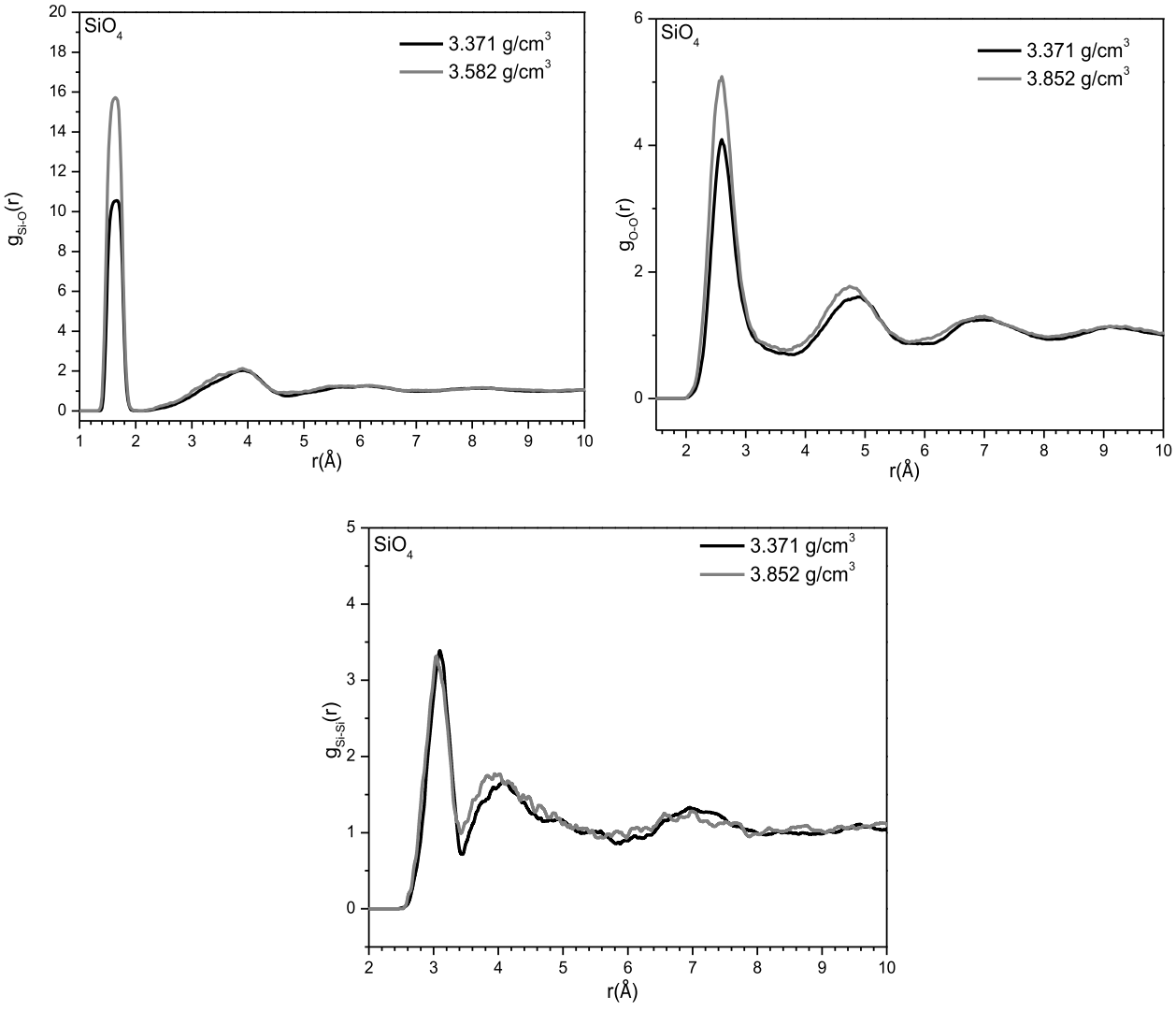

Fig. 3. The RDF of Si–O, O–O and Si–Si pairs in SiO_4 domain at different density.

the isolated SiO_4 units. The cluster with size of 9 atoms is the one comprising two SiO_4 units that link to each other via one bridging oxygen (BO). Similarly, the clusters with size from 13 to 77 atoms comprise from several to several tens SiO_4 units that link to each other via BO. The SiO_6 coordination units form small clusters with size from 7 to 72 atoms. The clusters with size of 7 atoms is the isolated SiO_6 units. The other SiO_6-clusters with larger size will comprise from several to several tens of SiO_6 units.

For model with density of $3.582\,g/cm^3$, the SiO_5 coordination units tend to form a very large cluster with size of 3549 atoms and four very small clusters with size from 6 to 21 atoms. The SiO_4 coordination units form the small clusters with size from 5 to 141 atoms. Similarly, the SiO_6 coordination units also form the small clusters with size from 7 to 152 atoms.

For model with density of $3.994\,g/cm^3$, the SiO_5 coordination units form the very large cluster with size of 3413 atoms and several ones with size of only one or two SiO_5 units. Similar, the SiO_6 coordination units also form a very large cluster with size of 3287 atoms, three small clusters are one isolated SiO_6 unit and two small clusters of 13 atoms (two SiO_6 units that link to each other via one BO). The SiO_4 coordination units form very small clusters with size from 5 to 21 atoms.

The above analysis reveals that the structure of amorphous silica is formed from SiO_4, SiO_5 and SiO_6 basic structure units. These basic structure units are not distributed uniformly in model, but tend to form SiO_4, SiO_5, SiO_6 clusters. In other word, the structure of amorphous silica consists of three structural phases: SiO_4-, SiO_5 and SiO_6-phases. At the density of $3.317\,g/cm^3$, the structure of amorphous silica mainly consists of two phases of SiO_4 and SiO_5, and one scattering phase of SiO_6 (the SiO_6 units form very small clusters and scatter in model so we call "scattering phase"). At density of $3.582\,g/cm^3$, the structure of amorphous silica consists of the main phase of SiO_5 and two scatting phases of SiO_4 and SiO_6. At $3.994\,g/cm^3$, the structure of amorphous silica consists of two main phases of SiO_5 and SiO_6, and one scattering phase of SiO_4. The intuitive snapshot of distribution

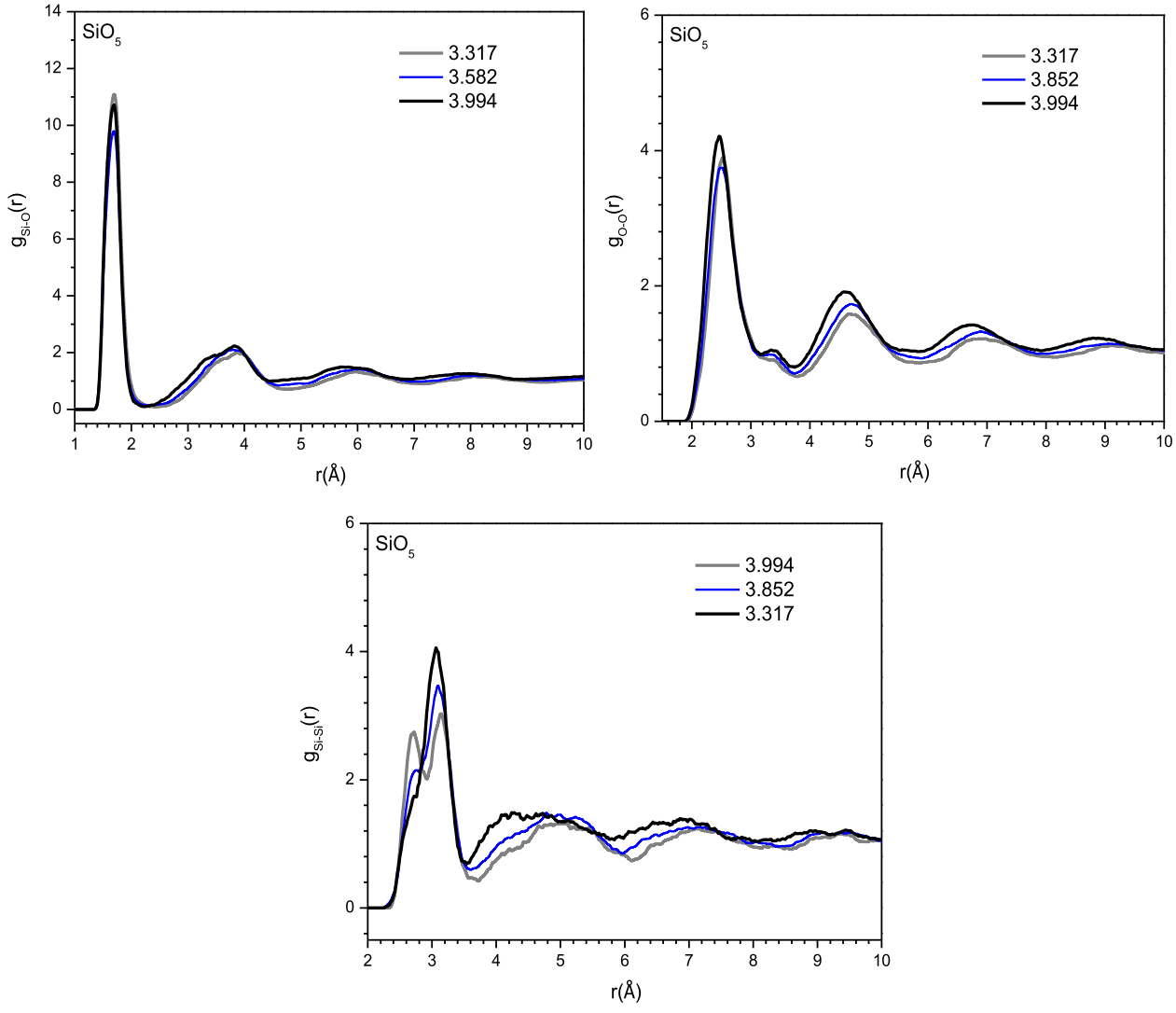

Fig. 4. The RDF of Si–O, O–O and Si–Si pairs in SiO_5 domain at different density.

Table 3. Distribution of the number of corner-sharing bonds, edge-sharing bonds, and face-sharing bonds. Here, Nc, Ne and Nf are the number of corner-sharing bonds, edge-sharing bonds, and face-sharing bonds respectively; Dc, De and Df are the average-distance of corner-sharing bonds, edge-sharing bonds, and corner-sharing bonds respectively.

Density (g/cm^3)	Nc	Ne	Nf	Dc (Å)	De (Å)	Df (Å)
3.317	4156	772	47	3.1527	2.7749	2.5728
3.582	4405	1179	114	3.1733	2.7746	2.5595
3.994	4892	1664	181	3.2007	2.7584	2.5536

of SiO_x-phases (SiO_x-domain) in 3D space is shown in Figure 2. The phase separation and forming the regions with different structures (polyamorphism) also has been referred in previous works [34,35,50]. However, the previous works have not calculated the size distribution of clusters (phase regions). In the view of grain structure, we can consider that each SiO_x-cluster is similar to a single crystalline grain in polycrystalline materials. So, the structure of amorphous silica is formed from SiO_4-, SiO_5- and SiO_6-grains. This reveals the polyamorphism in amorphous silica. The small clusters are located at boundary between grains (large clusters).

Now we will focus on clarifying the local and intermediate structure order of SiO_x-phases as well as the relationship between the structural characteristics and density of model. Figure 3 displays the PRDF of Si–O, O–O and Si–Si pairs in SiO_4-phase. It can be seen that the position of the first peak of PRDFs is almost not dependent on pressure. It reveals that the bond distances of Si–O, O–O and Si–Si pairs in SiO_4-phase is not dependent on density/pressure. In other word, the topology of SiO_4 units is identical at different densities [9,50]. Figure 4 shows the PRDFs of Si–O, O–O and Si–Si pairs in SiO_5-phase. The PRDF of Si–O pair is almost

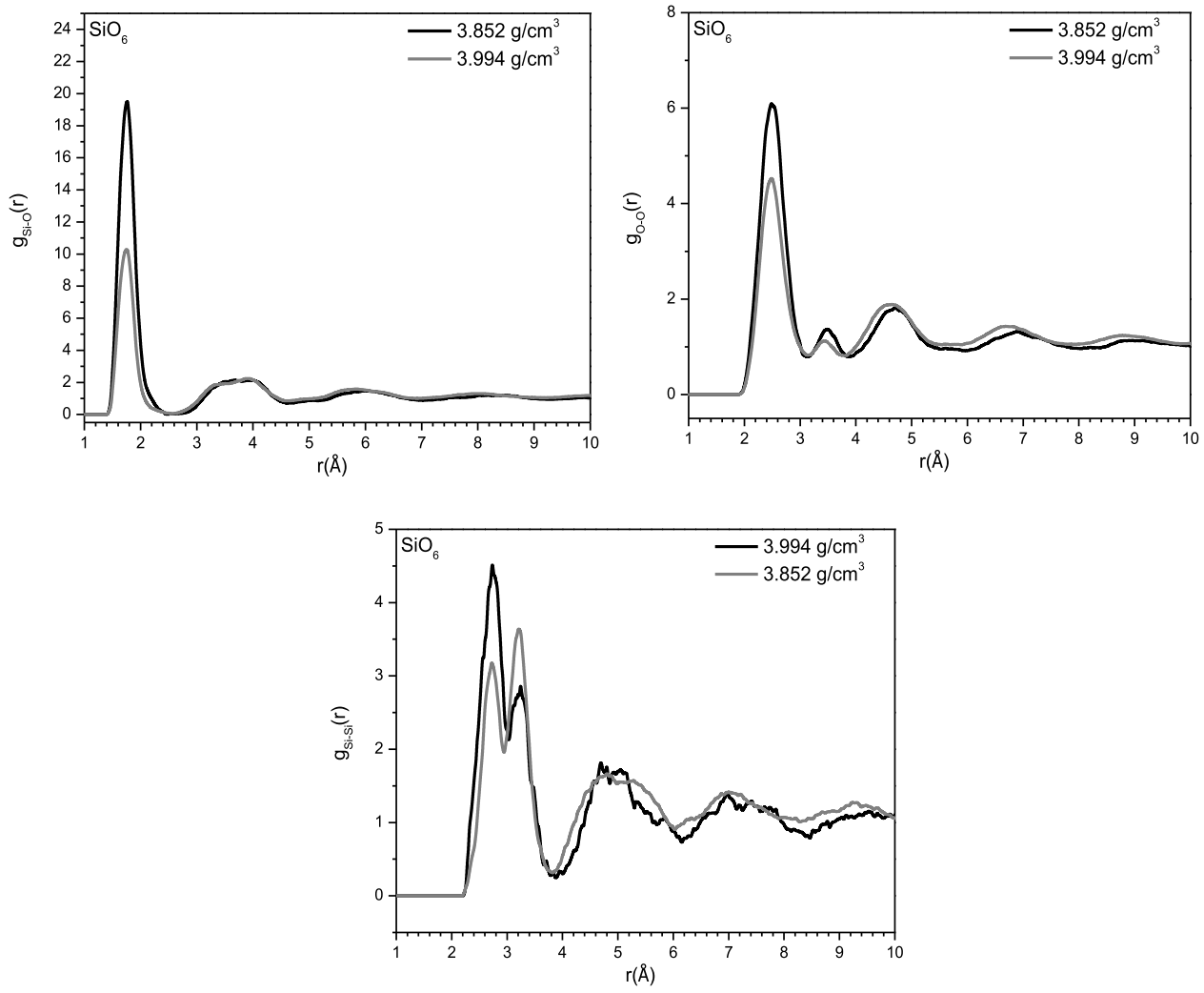

Fig. 5. The RDF of Si–O, O–O and Si–Si pairs in SiO_6 domain at different density.

not dependent on density, the PRDF of and O–O pair is slightly dependent on density. Meanwhile, PRDF of Si–Si pair is strongly dependent on pressure and the first peak of Si–Si PRDF splits into two peaks at high density. This reveals that topology of SiO_5 units at different density is identical but the connection between the SiO_5 units is strongly dependent on pressure. This can be explained as following: The SiO_5 units can link each other via one bridging oxygen (BO) that is called corner-sharing bonds, via two BOs that is called edge-sharing bonds, and three BOs that is called face-sharing bonds. The Si–Si bond distances in corner-sharing bonds, edge-sharing bonds, and face-sharing bonds are around 3.15–3.20 Å, 2.76–2.78 Å and 2.55–2.57 Å respectively, see Table 3.

The fraction of corner-, edge-, and face-sharing bonds increases strongly with pressure. As the fraction of edge-, and face-sharing bonds is small, the PRDF of Si–Si pair have a shoulder around position of 2.70–2.80 Å beside the main peak at around 3.15–3.20 Å. As the fraction of edge-, and face-sharing bonds increases, the first peak in PRDF of Si–Si pair splits in two small peaks. Similarly, Figure 5 shows the PRDFs of Si–O, O–O and Si–Si pairs in SiO_6 phase. It can be seen that the average Si–O, O–O bond distances are almost not changed with density. This demonstrates that the topology of SiO_6 at different densities is also identical. The first peak of PRDF of Si–Si pair is split in two peaks at location of around 2.76–2.78 and 3.15–3.20 Å. These locations correspond to the edge- and corner-sharing bond distances. This is also easy to understand because the number of face-sharing bonds is small in comparison with the number of corner- and edge-sharing bonds. Besides, the face-sharing bond distance (around 2.55–2.57 Å) is very close to the edge-sharing bond distance (2.76–2.78 Å). Two peaks corresponding edge- and face sharing bonds have merged into one peak at location of around 276–2.80 Å.

4 Conclusion

Structure of amorphous silica at different densities has been investigated by MD simulation. The results reveal that their structure comprises three phases: SiO_4-, SiO_5-, and SiO_6-phases. At density of 3.317 g/cm^3, the structure of amorphous silica mainly consists of two main phases of SiO_4 and SiO_5, and one scattering phase of SiO_6. As

density increases, the structure tends to transform from SiO_4 phase to SiO_6 phase. At density of $3.582\,g/cm^3$, the structure of amorphous silica comprises the main SiO_5-phase and the SiO_4 and SiO_6 scattering phases. At high density of $3.994\,g/cm^3$, its structure mainly consists of SiO_5- and SiO_6-phases and one scattering phase of SiO_4. The topology of SiO_x ($x = 4, 5, 6$) at different densities is identical. In the SiO_4-phase, the SiO_4 units link to each other via corner-sharing bonds with average Si–Si bond distance is around 3.15–3.20 Å. In the SiO_5- and SiO_6 phases, the SiO_5/SiO_6 units can link to each other by corner-, edge- and face-sharing bonds with average Si–Si bond distance are around 3.15–3.20 Å, 2.76–2.78 Å and 2.55–2.57 Å respectively. That is why the first peak of the Si–Si PRDF in SiO_5- and SiO_6-phases is split into two small peaks. In the view of considering the clusters of SiO_x are similar to grains of single crystalline in polycrystalline materials then the structure of amorphous silica is formed from SiO_4-, SiO_5- and SiO_6-grains. Boundary between grains are small clusters with size from several to several tens of SiO_x-units. This reveals the polyamorphism in amorphous silica that is the same as the concept of polymorphism for crystalline materials.

This research is funded by Vietnam National Foundation for Science and Technology Development (NAFOSTED) under grant number: 103.05-2018.38.

Author contribution statement

N.V. Hong conducted the models; N.V. Hong, L.T. Vinh, P.K. Hung, M.V. Dung, N.V. Yen analyzed data. N.V. Hong and L.T. Vinh wrote the manuscript. All authors discussed the results and contributed to the final manuscript.

References

1. A.R. Oganov, M.J. Gillan, G. David Price, Phys. Rev. B **71**, 064104 (2005)
2. V.P. Prakapenka, G. Shen, L.S. Dubrovinsky, M.L. Rivers, S.R. Sutton, J. Phys. Chem. Solids **65**, 1537 (2004)
3. R. Vuilleumier, N. Sator, B. Guillot, Geochim. Cosmochim. Acta **73**, 6313 (2009)
4. T. Tsuchiya, J. Tsuchiya, Proc. Natl. Acad. Sci. **108**, 4 (2011)
5. J. Geske, B. Drossel, M. Vogel, AIP Adv. **6**, 035131 (2016)
6. D.M. Teter, R.J. Hemley, G. Kresse, J. Hafner, Phys. Rev. Lett. **80**, 2145 (1998)
7. B.B. Karki, B. Dipesh, L. Stixrude, Phys. Rev. B **76**, 104205 (2007)
8. C. Prescher et al., Proc. Natl. Acad. Sci. **83**, 10041 (2017)
9. P.K. Hung, N.V. Hong, Eur. Phys. J. B **71**, 105 (2009)
10. L.T. San, N.V. Hong, P.K. Hung, High Pressure Res. **36**, 187 (2016)
11. P.K. Hung, N.V. Hong, L.T. Vinh, J. Phys.: Condens. Matter **19**, 466103 (2007)
12. Q. Mei, C.J. Benmore, J.K.R. Weber, Phys. Rev. Lett. **98**, 057802 (2007)
13. R.L. Mozzi, B.E. Warren, J. Appl. Cryst. **2**, 164 (1969)
14. D.I. Grimley, A.C. Wright, J. Non-Cryst. Solids **119**, 49 (1990)
15. A.C. Wright, J. Non-Cryst. Solids **179**, 84 (1994)
16. P.F. Mcmillan, B.T. Poe, Ph. Gillet, B. Reynard, Geochim. Cosmochim. Acta **58**, 3653 (1994)
17. R.G. Della Valle, H.C. Andersen, J. Phys. Chem. **97**, 2682 (1992)
18. S. Munetoh, T. Motooka, K. Moriguchi, A. Shintani, Comput. Mater. Sci. **39**, 334 (2007)
19. A. Kerrache, V. Teboul, A. Monteil, Chem. Phys. **321**, 69 (2006)
20. A. Takada, P. Richet, C.R.A. Catlow, G.D. Price, J. Non-Cryst. Solids **345–346**, 224 (2004)
21. P.H. Poole, M. Hemmati, C.A. Angell, Phys. Rev. Lett. **79**, 2281 (1997)
22. I. Saika-Voivod, F. Sciortino, P.H. Poole, Phys. Rev. E **63**, 011202 (2000)
23. T. Sato, N. Funamori, Phys. Rev. Lett. **101**, 255502 (2008)
24. T. Sato, N. Funamori, Phys. Rev. B **82**, 184102 (2010)
25. J. Sarnthein, A. Pasquarello, R. Car, Phys. Rev. B **52**, 12690 (1995)
26. A. Trave, P. Tangney, S. Scandolo, A. Pasquarello, R. Car, Phys. Rev. Lett. **89**, 245504 (2002)
27. A. Takada, J. Non-Cryst. Solids **499**, 309 (2018)
28. J.R. Rustad, D.A. Yuen, Phys. Rev. B **44**, 2108 (1991)
29. P.K. Hung, L.T. Vinh, T. Ba Van, N.V. Hong, N.V. Yen, J. Non-Cryst. Solids **462**, 1 (2017)
30. L.S. Dubrovinsky, N.A. Dubrovinskaya, S.K. Saxena, F. Tutti, S. Rekhi, T.L. Bihan, G. Shen, J. Hu, Chem. Phys. Lett. **333**, 264 (2001)
31. D. Andrault, G. Fiquet, F. Guyot, M. Hanfland, Science **282**, 720 (1998)
32. D. Andrault, R.J. Angel, J.L. Mosenfelder, T.L. Bihan, Am. Miner. **88**, 301 (2003)
33. I. Saika-Voivod, F. Sciortino, T. Grande, P.H. Poole, Phys. Rev. E **70**, 061507 (2004)
34. I. Saika-Voivod, F. Sciortino, P.H. Poole, Phys. Rev. E **63**, 011202 (2001)
35. D.J. Lacks, Phys. Rev. Lett. **84**, 4629 (2000)
36. O. Mishima, L.D. Calvert, E. Whalley, Nature **314**, 76 (1985)
37. O. Mishima, K. Takemura, K. Aoki, Science **254**, 406 (1991)
38. O. Mishima, J. Chem. Phys. **100**, 5910 (1994)
39. K. Winkel, M.S. Elsaesser, E. Mayer, T. Loerting, J. Chem. Phys. **128**, 044510 (2008)
40. T. Loerting, N. Giovambattista, J. Phys.: Condens. Matter **18**, R919 (2006)
41. P. Gallo et al., Chem. Rev. **116**, 7463 (2016)
42. M. Grimsditch, Phys. Rev. Lett. **52**, 2379 (1984)
43. R.J. Hemley, H.K. Mao, P.M. Bell, B.O. Mysen, Phys. Rev. Lett. **57**, 747 (1986)
44. E. Lascaris, M. Hemmati, S.V. Buldyrev, H. Eugene Stanley, C. Austen Angell, J. Chem. Phys. **140**, 224502 (2014)
45. E. Lascaris, Phys. Rev. Lett. **116**, 125701 (2016)
46. R. Chen, E. Lascaris, J.C. Palmer, J. Chem. Phys. **146**, 234503 (2017)
47. M.S. Somayazulu et al., J. Phys.: Condens. Matter **5**, 6345 (1993)
48. J.S. Tse, D.D. Klug, Y. LePage, Phys. Rev. B **46**, 5933 (1992)
49. W. Jin, R.K. Kalia, P. Vashishta, J.P. Rino, Phys. Rev. Lett. **71**, 3146 (1993)
50. N.V. Hong, M.T. Lan, N.T. Nhan, P.K. Hung, Appl. Phys. Lett. **102**, 191908 (2013)